

Multichannel scattering theory of the resonant Auger effect in photoelectron spectroscopy

Françoise Combet Farnoux

*Laboratoire Spectroscopie Atomique et Ionique,
Université Paris-Sud; Bâtiment 350-91405, Orsay, France*

(Received 18 June 1981)

Photoelectron spectroscopy has allowed us recently to observe both giant resonance enhancement of primary lines and two-electron resonant Auger satellites corresponding to the resonant behavior of photoemission cross sections relative, respectively, to autoionization and Auger decay channels. Using multichannel scattering theory and configuration-interaction formalism, I have established general formulas to parametrize the photoemission cross sections in the neighborhood of nonradiatively decaying excited states located near inner-shell ionization thresholds. Considering both cases of one isolated resonance and n -resonant states decaying into N continua, I have shown why the two types of decay (autoionization and Auger) cannot be treated independently and have stressed the importance of coupling autoionization channels with Auger ones to account for the asymmetry profile of Auger partial cross sections and the presence of extra structures due to neighboring resonances in Auger channels. Some examples are discussed to point out that the relative importance of primary and satellite lines may vary strongly with the element and the energy range considered. The determination of the parameter $\alpha_n(\mu E)$ typical of a resonance n in each channel μ provides us with many types of information, such as the importance of interchannel coupling, spin-orbit effects, and the existence of shake-up satellites.

I. INTRODUCTION

During these last years, the fast development of VUV photoelectron and photoemission spectroscopies has allowed to observe remarkable features in the core-level spectra relevant to the VUV energy range. We note that, because of a different position of the threshold for vapor and solid-state samples, some so-called "threshold effects" in solid-state physics can be observed below the corresponding ionization thresholds in atomic physics, but I will focus here on the atomic case. I will consider such energy range that resonant absorption lines appear in photoabsorption spectra between the ionization thresholds corresponding to two adjacent inner subshells. From the point of view of photoelectron spectroscopy, this means that the photoelectron may be captured into bound excited states likely to decay nonradiatively into open channels, via autoionization and Auger processes. When each of these two processes leads to different ionic final states, i.e., different decay channels, we will distinguish autoionization channels which contribute to lines of the primary spec-

trum and Auger channels which allow to observe satellite lines. The former ones will be called here primary lines in contrast with the second ones, and I shall show in this paper that both types of decay cannot be treated independently as each one is modified by the presence of the other one; also, both types of lines are likely to be resonant for a photon energy close to the position of the decaying excited state. The recent theoretical work of Combet Farnoux and Ben Amar¹ relative to the M_{23} spectrum of Ni^+ has shown the importance of such a mechanism: Several resonant series converging on the various $3p$ ionization thresholds may decay by both autoionization into channels coming from a single $3d$ -electron ionization and Auger process (super-Coster-Krönig transition) into several channels opened by simultaneous ionization and excitation (shake-up process) of the $3d$ subshell.

Although the observation of these resonant satellite lines is pretty recent in photoelectron spectroscopy, the importance of the Auger decay of excited states belonging to series below inner-shell thresholds had been reported for krypton and xenon as

soon as 1965 by Fano and Cooper,² and tentatively treated by Mies³ from scattering formalism, but this author who especially focused on the total photoabsorption cross section was conscious that a real treatment would require the knowledge of partial cross sections in each channel, as given by photoelectron spectroscopy. Using synchrotron radiation as a tunable light source, Eberhardt *et al.*⁴ have analyzed the $N_{45}O_{23}O_{23}$ Auger spectrum of xenon and the $M_{45}N_{23}N_{23}$ Auger spectrum of krypton when the atom is excited to photon energies around the respective $4d$ - and $3d$ -ionization threshold values; they especially emphasize the observation of a shift of the $N_{45}O_{23}O_{23}$ ($M_{45}N_{23}N_{23}$) Auger multiplet structure to higher kinetic energy after excitation to the $6p$ (Xe) and $5p$ (Kr) resonance line, as a probe of core rearrangement and other correlation effects in Auger transitions, but no quantitative relation between these Auger satellites and the Xe $5s$ (and Kr $4s$) lines of the directly emitted photoelectrons has been reported. More recently, Chandesris *et al.*⁵ have observed three Auger satellite lines, in addition to the primary $3d$ lines, in photoemission studies of copper vapor; all lines resonate at the vicinity of the location of the $3p^5 3d^{10} 4s^2$ excited state below $3p$ thresholds. Calculations for copper are in progress⁶; they require the coupling of many channels (opened by both single $3d$ and $4s$ ionization and simultaneous $3d$ ionization and excitation) with one another and with several excited states involving a $3p$ hole. The general theory of such a complicated case has been presented by Starace⁷ for as complex systems as the lanthanides, but no numerical application

has been yet achieved for open-shell systems, and more particularly, when Auger decay of the excited states is more important than direct autoionization.

The main and original purpose of this paper consists in presenting a general and unified theory of the resonant behavior of both primary and Auger satellite lines observed in photoelectron spectroscopy when scanning the energy range below an inner-shell ionization threshold. As such, it is an extension of the Starace⁸ paper which was devoted to the behavior of partial cross sections and branching ratios in the neighborhood of a resonance without any reference to Auger decay and the possibility of the overlapping of several resonances, two events likely to show up in case of inner-shell excitation. This is why, as a starting point and in contrast with Starace, I will focus first on the determination in each channel, of the resonant wave function taking into account the interaction of n -discrete excited states with many continua. Within this purpose, Sec. II will follow closely Mies³ the approach of which is a generalization of the Fano⁹ configuration-interaction theory. In Sec. III, I will establish various formulas displaying the resonant behavior of the dipole matrix elements and the photoemission cross sections, and I will distinguish Auger decay and direct autoionization channels according to the value of a parameter $\alpha(\mu E)$, characteristic of each channel μ . This study will clearly stress why theoretical models neglecting first-order interchannel interactions may be not appropriate to point out the asymmetrical character of resonant lines in Auger channels observed in photoelectron spectroscopy.

II. SUMMARY REVIEW OF THE INTERACTION BETWEEN MANY DISCRETE STATES AND MANY CONTINUA

Let us remark that, although in this section we have in mind photoionization of atoms and ions, the formulas presented apply also to inelastic electron scattering from atoms and ions, and could be easily extended to the same problems in molecules. In fact, we are seeking first the set of degenerate, orthonormal ($N^0 + 1$) electron continuum wave functions $\psi_{\mu E}^-$ with total energy E , which describe the interaction of a free electron with an N^0 electron ion. They describe an observable channel μ and are the exact incoming-wave eigenfunctions of the Hamiltonian H ; their asymptotic behavior must be that of an outgoing wave in channel μ with incoming waves in all channels, normalized per unit energy range, according to

$$\psi_{\mu E}^- = \sum_{\mu'} \mathcal{F}_{\mu'} \left[\frac{2}{\pi k_{\mu}(E)} \right]^{1/2} \frac{1}{r} [\exp(i\theta_{\mu'}) \delta_{\mu\mu'} - S_{\mu\mu'}^\dagger \exp(-i\theta_{\mu'})], \quad (1)$$

with

$$\theta_{\mu} = k_{\mu} r - \frac{1}{2} l_{\mu} \pi - \frac{Z - N^0}{k_{\mu}} \ln(2k_{\mu} r) + \arg \Gamma[l_{\mu} + 1 - i(Z - N^0)/k_{\mu}]. \quad (2)$$

Here \mathcal{F} comprises the wave function of the ionic core and the appropriate angular factors; k_{μ} is the wave

number of an electron ejected with angular momentum l_μ in the μ channel related to the total energy E , and the μ th ionization potential E_μ by

$$k_\mu(E) = [2m(E - E_\mu)]^{1/2} / \hbar. \quad (3)$$

The matrix S^\dagger is the adjoint of the scattering matrix in the angular momentum representation.

A. Choice of basis states (discrete and continuum)

Following Fano⁹ and Mies³ we start with n -orthogonal prediagonalized discrete states $|F_n\rangle$ and a set of N -orthogonal prediagonalized continuum states $|\beta E\rangle$, where β indicates a set of channel quantum numbers and E the total energy of the state. This means that these wave functions diagonalize separate submatrices of H :

$$\langle \beta' E' | H - E | \beta'' E'' \rangle = (E' - E) \delta_{\beta' \beta''} \delta(E'' - E'), \quad (4)$$

$$\langle F_n | H - F | F_m \rangle = (E_n - E) \delta_{nm}, \quad (5)$$

while $V_{n\beta}(E, E')$ represents the off-diagonal terms which couple the subsets $\{n\}$ and $\{\beta, E'\}$, i.e., the discrete-continuum interaction:

$$\langle \beta E | H - E | F_n \rangle = V_{n\beta}(E, E'). \quad (6)$$

In other words, the $|\beta E\rangle$ states defined by (4) are obtained by diagonalizing the submatrix of H defined by the N open continuum channels whose observable states are represented by $|\mu E\rangle$. We refer to the paper of Starace⁷ for details of this diagonalization, but before treating the second step, the diagonalization of the discrete-continuum interaction, we recall that these prediagonalized states may be written

$$|\beta E\rangle = \sum_\mu \left[|\mu E\rangle + \sum_{\mu'} P \int dE' \frac{\langle \mu' E' | K^0(E) | \mu E \rangle}{E - E'} \right] T_{\mu\beta}(E) \cos \eta_\beta \quad (7)$$

in terms of the asymptotically observable states $|\mu\rangle$ of the ion-electron system which are not eigenstates of H . $|\beta E\rangle$ is a standing wave so that the configuration-interaction matrix element $V_{n\beta}$ is real in (6). β is a degeneracy index and does not stand for any physical channel. In (7), $\langle \mu' E' | K^0(E) | \mu E \rangle$ is the reactance matrix of collision theory. P indicates that the Cauchy principal part must be taken when integrating over the singularity of the denominator. The T matrix is a real orthogonal matrix which diagonalizes both the scattering matrix S^0 and the on-the-energy-shell reactance matrix K^0 . The η_β are eigenphases and together with T define S^0 and K^0 :

$$S^0 = \tilde{T} e^{2i\eta} T = (I - iK^0)(I + iK^0)^{-1}, \quad (8)$$

$$K^0 = \tilde{T}(-\tan \eta) T = i(I - S^0)(I + S^0)^{-1}, \quad (9)$$

I being the unit matrix. So, we can write the asymptotic form of $|\beta E\rangle$:

$$\sum_\mu \mathcal{F}_\mu \left[\frac{2}{\pi k_\mu(E)} \right]^{1/2} \left[\frac{1}{r} \right] \sin(\theta_\mu + \eta_\beta) T_{\mu\beta} \quad (10)$$

with the same notations as in (1). It is useful to define a matrix A^0 by formulas:

$$A^0 = e^{i\eta} T, \quad (11)$$

$$A^{0*} \tilde{A}^0 = \tilde{A}^{0*} A^0 = 1,$$

and also to stress that, far from resonance, the wave function describing a particular channel μ is written

$$\psi_{\mu E}^0 = \sum_\beta e^{-i\eta_\beta} T_{\beta\mu} |\beta E\rangle = \sum_\beta A_{\beta\mu}^{0*} |\beta E\rangle. \quad (12)$$

B. Determination of the set of $\psi_{\mu E}^-$ states

Starting with the two subsets of prediagonalized states defined above, in the case of many discrete states interacting with many continua, we must use a linear combination of the two sets to represent the exact total wave function $\psi_{\mu E}^-$ in each channel μ at total energy E :

$$\psi_{\mu E}^- = \sum_n B_{\mu n}(E) |F_n\rangle + \sum_\beta \int dE' C_{\mu\beta}(E, E') |\beta E'\rangle. \quad (13)$$

We refer the reader to the paper of Mies³ for the detailed calculations relative to the diagonalization of the residual discrete-continuum interaction defined in (6), and we will mention here only the formulas necessary for the understanding and the cohesion of the present paper. To make $\psi_{\mu E}^-$ an eigenstate of H with eigenvalue E , we obtain

$$C_{\mu\beta}(E, E') = P \left[\frac{Y_{\mu\beta}(E, E')}{E - E'} \right] + Z_{\mu\beta}(E) \delta(E - E'), \quad (14)$$

where $Z_{\mu\beta}$ is an arbitrary function of E , and

$$Y_{\mu\beta}(E, E') = B_{\mu n}(E) V_{n\beta}(E, E'). \quad (15)$$

The following coupled equations must be solved to obtain the $B_{\mu n}$:

$$EB_{\mu n} - \sum_m D_{mn} B_{\mu m} = \sum_\beta Z_{\mu\beta} V_{n\beta}, \quad (16)$$

where $D_{nm}(E)$ is a symmetric real matrix:

$$D_{mn}(E) = E_n \delta_{nm} + P \int dE' \frac{1}{E - E'} \sum_\beta V_{m\beta}(E, E') V_{n\beta}(E, E'). \quad (17)$$

Before solving explicitly (16) we have to replace the $|F_n\rangle$ states by a new set of orthogonal states $|\Phi_n\rangle$ diagonalizing the D matrix. The positions \bar{E}_n of these new states are given by the eigenvalues of D , so that G being a real and orthogonal matrix defines the transformation

$$|\Phi_n\rangle = \sum_m G_{nm} |F_m\rangle. \quad (18)$$

We obtain a new configuration-interaction matrix $W_{n\beta}(E, E')$ related to the matrix $V_{n\beta}(E, E')$ by

$$W_{n\beta}(E, E') = \langle \beta E' | H - E | \Phi_n \rangle = \sum_m G_{nm} V_{m\beta}(E, E') \quad (19)$$

so that both coefficients $\bar{B}_{\mu n}$ of the new states Φ_n (in the development of $\psi_{\mu E}^-$, where $[\bar{B}] = [B][\tilde{G}]$), and new $Y_{\mu\beta}(E, E')$ as defined in (15) are proportional to a new $[Z]$ matrix, the coefficient matrices being $[W_{n\beta}]$ for the $B_{\mu n}$ and the new matrix $[K]$ for the $[Y_{\mu\beta}]$ matrix. As usual, notation $W_{n\beta}$ is used for the on-the-energy-shell terms ($E' = E$) of the $n \times N$ matrix $W_{n\beta}(E)$, while $W_{n\beta}(E, E')$ indicates the dependence on energy (E, E'). In the same way, we define the on-the-energy-shell $N \times N$ reactance matrix $K(E)$ by

$$K_{\beta\beta'}(E) = \sum_n \frac{\pi W_{n\beta} W_{n\beta'}}{E - \bar{E}_n}, \quad (20)$$

so that expression (13) of $\psi_{\mu E}^-$ may be written

$$\psi_{\mu E}^- = \sum_\beta Z_{\mu\beta} \left[\sum_n \frac{W_n}{E - E_n} |\bar{\Phi}_n\rangle + |\beta E\rangle \right], \quad (21)$$

$$\bar{\Phi}_n = \Phi_n + \sum_\beta P \int \frac{dE'}{E - E'} W_{n\beta}(E, E') |\beta E'\rangle, \quad (22)$$

this modified resonance state $\bar{\Phi}_n$ including an admixture of continuum states according to Fano's paper.⁹

In order to use (21) in our study, we have to determine the normalization matrix $[Z]$: Imposing the asymptotic behavior of (1) to expression (13) of $\psi_{\mu E}^-$ and after substituting Eq. (14) for $C_{\mu\beta}$ and expressing $|\beta E'\rangle$ in terms of its asymptotic behavior (10) with its associated matrices $[T]$ and $[A^0]$, I have shown, with matrix notation:

$$[I] = [Z][I - iK][A^0], \quad (23)$$

$$[S]^\dagger = [Z][I + iK][A^0]^*, \quad (24)$$

$[I]$ being the unit matrix, so that

$$[Z] = [A^0]^{-1} [I - iK]^{-1}. \quad (25)$$

C. Change of the continuum states basis

In case of a single resonance, it is always possible to transform the N -degenerate continua $|\beta E\rangle$ to a new set of N -orthonormal diagonalized contin-

uum states such as only a single member interacts with the discrete state $|F_1\rangle$. If $|\lambda E\rangle$ represents this new set such as

$$\langle \lambda E | \lambda' E' \rangle = \delta(\lambda, \lambda') \delta(E - E'), \quad (26)$$

$$\langle \lambda E | H | \lambda' E' \rangle = E \delta(\lambda, \lambda') \delta(E - E'), \quad (27)$$

the single continuum state $|1E\rangle$ belongs to a channel which then interacts with the discrete state as if the other $N - 1$ continuum channels were not there and formed a background unaffected by the resonance. We refer, for this transformation, to the Fano⁹ paper and the more recent work of Starace⁸ which gives a review of it. However, we must recall properties involving this new set, in so far as they will be useful in the following part of this paper. In fact, since no transition is possible between $|F_1\rangle$ and the $|\lambda E\rangle$ with $2 \leq \lambda \leq N$, these diagonalized states are eigenstates $|\lambda E\rangle$ of H (we use the notation with rounded bras and kets to refer to eigenstates). Another exact standing wave eigenfunction $|1E\rangle$ is obtained as a linear combination of only $|F_1\rangle$ and $|1E\rangle$ according to

$$|1E\rangle = \frac{\sin(-\Delta)}{\pi V_t} |\bar{F}_1\rangle + \cos(-\Delta) |1E\rangle, \quad (28)$$

with

$$\tan(-\Delta) = \frac{1}{\epsilon} = \frac{\pi V_t^2}{E - \bar{E}_1} = \frac{\frac{1}{2}\Gamma_t}{E - \bar{E}_1}, \quad (29)$$

$$|\bar{F}_1\rangle = |F_1\rangle + P \int \frac{dE'}{E - E'} V_t |1E\rangle, \quad (30)$$

$$\bar{E}_1 = E_1 + P \int \frac{dE'}{E - E'} V_t^2. \quad (31)$$

Since $|1E\rangle$ involves the whole interaction with the resonance, V_t defines the total linewidth Γ_t via the relations

$$\frac{1}{2}\Gamma_t = \pi V_t^2 = \pi \langle 1E | H | F_1 \rangle^2 = \pi \sum_{\beta} V_{1\beta}^2, \quad (32)$$

$$|1E\rangle = \frac{1}{V_t} \sum_{\beta} V_{1\beta} |\beta E\rangle, \quad (33)$$

and $|0\rangle$ being the ground state of the system before photoionization, we recall the expression giving q , the profile index of the resonance in the absorption spectrum, with Q representing the dipole transition operator:

$$q = \frac{\langle F_1 | Q | 0 \rangle}{\pi \langle 1E | H | F_1 \rangle \langle 1E | Q | 0 \rangle}. \quad (34)$$

The other $|\lambda E\rangle$ ($\lambda \neq 1$) are simply linear combinations of $|\beta E\rangle$ states, the coefficients being determined by the unitary matrix which transforms the prediagonalized states $|\beta E\rangle$ into eigenvectors $|\lambda E\rangle$ which have no interaction with the discrete state.

III. RESONANT BEHAVIOR OF VARIOUS LINES IN INNER-SHELL PHOTOELECTRON SPECTROSCOPY

After the brief review of Sec. II, we have on hand the necessary formalism to study the resonant behavior of any partial cross section likely to be measured by photoelectron spectroscopy and photoemission, not only in the often invoked case of one isolated autoionizing resonance (see, for instance, the Starace⁸ paper or the work of Kabachnik and Sazhina¹⁰ relative to angular distribution and polarization of photoelectrons), but also when this resonance decays via simultaneous autoionization and Auger effect, as mentioned in the introduction. Also, the more complicated case where many resonances can be coupled among themselves via decay continua should be taken up within this framework: This latter event, with overlapping effects complicating the parametrization of the partial cross section in each channel, may be encountered when we are dealing with open-shell systems with large multiplet splitting effects. The number of open channels as well as that of resonance families are both increasing simultaneously, since when an atom (or ion) is photoionized, the residual ion may be left in any number of term levels, each possibly having a number of fine-structure levels.

However, since we are especially interested here in inner-shell excitation and ionization, this case of an isolated resonance deserves further attention, especially as the authors mentioned above have not taken into consideration the possibility of an Auger decay prevailing over direct autoionization. Moreover, as emphasized previously,¹¹ the existence of an effective potential barrier may let only one highly localized state show up strongly in inner-shell absorption spectra while excluding Rydberg and near-continuum states from overlapping with the inner shells from which excitation takes place. An illustration of this type of excitation is the $M_{4,5}$ spectra of the rare earths: In these spectra, the dominant features are the $3d_{5/2,3/2} \rightarrow 4f$ lines occurring below the $M_{4,5}$ thresholds, while transitions to the Rydberg and continuum states held outside the barrier are inhibited. Consequently, Sec. III A will be devoted to this case of an isolat-

ed resonance, while Sec. III B will develop the theoretical treatment of the resonant behavior of partial cross sections when no effective potential barrier prevents series of Rydberg states from converging to the same (or slightly displaced) ion limits. In both parts, I shall discuss the different types of behavior and shape (asymmetrical or not) of the resonant lines in any channel, in terms of the importance of interchannel coupling effects and parameter $\alpha_n(\mu E)$ characteristic of the resonance and the channel considered. A quantitative illustration of the importance of Auger decay will be provided by some numerical results obtained for copper⁶ in the same approximations as for the Ni⁺ case.¹²

A. Resonant behavior of any partial cross section near an isolated resonance

We shall start from the general formula (21) obtained above and relative to the wave function $\psi_{\mu E}^-$ describing an observable channel, in contrast with other authors^{8,10} who considered the incoming-wave-normalized final states under the form of a linear combination of standing-wave eigenfunctions $|\lambda E\rangle$, whose coefficients were obtained by application of the boundary conditions.

1. General case of many decay continua

Starting from (21) requires to determine the normalization matrix $Z_{\mu\beta}$, which is feasible directly in this relatively simple case. According to (25), the $(I - iK)$ matrix can be inverted easily and we find

$$[Z] = [A^0]^{-1} \left[I + iK \frac{\epsilon}{\epsilon - i} \right], \quad (35)$$

which may be written, using (20) and (29),

$$Z_{\mu\beta} = \sum_{\beta'} A_{\beta'\mu}^{0*} \left[\delta_{\beta\beta'} + i \frac{V_{1\beta} V_{1\beta'}}{V_t^2} \frac{1}{\epsilon - i} \right], \quad (36)$$

and allows to develop (21) under the form

$$\begin{aligned} \psi_{\mu E}^- = & \sum_{\beta} \left[A_{\beta\mu}^{0*} + i \frac{V_{1\beta}}{V_t} \frac{1}{\epsilon - i} \sum_{\beta'} A_{\beta'\mu}^{0*} \frac{V_{1\beta'}}{V_t} \right] \\ & \times \left[\frac{V_{1\beta}}{E - \bar{E}_1} |F_1\rangle + |\beta E\rangle \right]. \quad (37) \end{aligned}$$

Using the relations (6), (12), (29), (33), and the following ones:

$$H_{\mu} = \langle \psi_{\mu E}^0 | H | F_1 \rangle = \sum_{\beta'} A_{\beta'\mu}^0 V_{1\beta'}, \quad (38)$$

$$\begin{aligned} |\langle 1E | H | F_1 \rangle|^2 = & V_t^2 = \sum_{\beta} V_{1\beta}^2 = \sum_{\mu} |H_{\mu}|^2 \\ = & (1/2\pi) \sum \Gamma_{\mu}, \quad (39) \end{aligned}$$

we can write (37) under the more compact form

$$\psi_{\mu E}^- = \psi_{\mu E}^0 + \frac{H_{\mu}^*}{V_t} \left[\frac{|F_1\rangle}{\pi V_t} + i |1E\rangle \right] \frac{1}{\epsilon - i}. \quad (40)$$

If $Q_{\mu}^0 = \langle \psi_{\mu E}^0 | Q | 0 \rangle$ and using q as given by (34), it is easy to write the dipole transition matrix element $Q_{\mu} = \langle \psi_{\mu E}^- | Q | 0 \rangle$:

$$Q_{\mu} = Q_{\mu}^0 + \frac{H_{\mu} q - i}{V_t \epsilon + i} \langle 1E | Q | 0 \rangle, \quad (41)$$

and as a consequence of various unitary transformations:

$$\begin{aligned} V_t \langle 1E | Q | 0 \rangle = & \sum_{\beta} \langle F_1 | H | \beta E \rangle \langle \beta E | Q | 0 \rangle \\ = & \sum_{\mu} \langle F_1 | H | \psi_{\mu E} \rangle \langle \psi_{\mu E} | Q | 0 \rangle, \quad (42) \end{aligned}$$

hence

$$\langle 1E | Q | 0 \rangle = \frac{1}{V_t} \sum_{\mu} H_{\mu}^* Q_{\mu}^0, \quad (43)$$

and Q_{μ} is taking the general alternative form

$$\begin{aligned} Q_{\mu} = & Q_{\mu}^0 \left[1 + \frac{\Gamma_{\mu} q - i}{\Gamma_t \epsilon + i} \right] \\ & + 2\pi \frac{H_{\mu} q - i}{\Gamma_t \epsilon + i} \sum_{\mu' \neq \mu} H_{\mu'}^* Q_{\mu'}^0. \quad (44) \end{aligned}$$

Formulas (41) and (43) are equivalent to an expression given by Starace⁸ in his recent paper [formula (25)] where he defines a quantity $\alpha(\mu E)$ representing the fraction of the dipole amplitude Q_{μ}^0 that passes through the eigenchannel $|1E\rangle$. In fact, expression (24) in the Starace⁸ paper is equivalent in our notation to

$$\alpha(\mu E) Q_{\mu}^0 = \frac{H_{\mu}}{V_t} \langle 1E | Q | 0 \rangle, \quad (45)$$

which allows us to write

$$Q_{\mu} = Q_{\mu}^0 \left[1 + \alpha(\mu E) \frac{q - i}{\epsilon + i} \right]. \quad (46)$$

Considering any expression of Q_μ as given by (41), (44), and (46), we obtain the following important conclusions.

(1) Q_μ is the sum of a resonant part which has the same energy dependence for all channels via ϵ and a background contribution Q_μ^0 representing the dipole amplitude far from resonance.

(2) q and ϵ are the parameters defined in photo-absorption according to formulas (34) and (29) above. The partial cross section in each channel μ is proportional to $|Q_\mu|^2$, and using any expression of Q_μ we obtain

$$\sigma_\mu \propto |Q_\mu^0|^2 \left[1 + |\alpha|^2 \frac{q^2 + 1}{\epsilon^2 + 1} + 2 \operatorname{Re} \alpha \frac{\epsilon q - 1}{\epsilon^2 + 1} + 2 \operatorname{Im} \alpha \frac{\epsilon + q}{\epsilon^2 + 1} \right]. \quad (47)$$

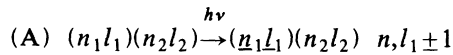
According to this general formula, and if α takes a finite value, σ_μ corresponds to an asymmetrical profile, since the numerator of (47) contains ϵ only in the first power so that it is possible to transform the parentheses in (47) into the sum of a constant term and a Fano resonance:

$$\sigma_\mu \propto |Q_\mu^0|^2 \left[(1 - a_\mu^2) + a_\mu^2 \frac{(\bar{q}_\mu + \epsilon)^2}{\epsilon^2 + 1} \right], \quad (48)$$

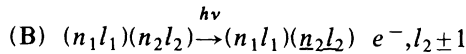
\bar{q}_μ defining the profile index of the resonance in

2. Resonant Auger effect

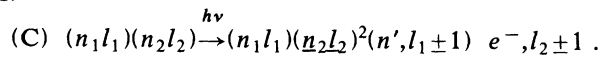
A major interest of the formulas in Sec. III A 1 above lies in their generality. In fact, they are suitable for describing the resonant behavior in any channel which an excited state decays into, via direct autoionization or Auger process, provided α is not zero or infinite. By direct autoionization, we mean interference between the following excitation process (A) with the underlined notation indicating a hole state:



and the following ionization process (b);



while Auger decay (autoionization of the inner core) represents the interference between the same excitation and another ionization process (C) accompanied by a shake-up excitation, leading to a two-hole state, as follows:



We refer to (C) as an Auger process since the final state of the system differs from the initial one by two one-electron excitations; $n' = n$, i.e., the outer electron left undisturbed is the most likely event,

this μ channel, both \bar{q}_μ and a_μ^2 can be expressed in terms of α and q .

Let us consider some interesting limit cases

(a) $\alpha(\mu E) = 0$ because $H_\mu = 0$ corresponds to the continuum channels where there is no decay of the resonance and $\sigma_\mu \propto |Q_\mu^0|^2$.

(b) $\alpha(\mu E)$ infinite with $Q_\mu^0 = (\langle 1E | Q | 0 \rangle \neq 0)$ corresponds to Auger decay channels whose coupling with the direct autoionization channels has not been taken into account or is quite negligible; we shall return below to this case which leads to Lorentzian resonant profiles in the corresponding Auger decay channels, insofar as it stresses an important result: *Asymmetry of resonant lines in Auger channels is due essentially to interchannel effects*, when coupling both direct autoionization and Auger decay channels to obtain the $|\beta E\rangle$ states in Sec. II. The following sections (III A 2 and III A 3) below will help to make this point more explicit.

(3) Starting from (47) and using (42), it would be straightforward to sum σ_μ over all channels μ and to obtain the well-known total cross section σ_t , whose parametrization has been explicated by Fano.⁹

(4) In (39) and (44) we have introduced a partial linewidth Γ_μ , but we must recall that it corresponds to no observed linewidth and lifetime; \hbar/Γ_t corresponds to the lifetime of the resonant excited state considered, and only the total linewidth $\Gamma_t = \sum_\mu \Gamma_\mu$ is observed in any channel.

but $n' \neq n$ may occur in (C) as a by-product of the inner core's further ionization, giving rise to a double Auger event which has been observed in recent experiments on Xe and Kr.⁴ This resonant double

Auger process can be considered a special case of Auger process generating two continuum electrons and observed by Krause and Carlson¹³ as early as 1966. Indeed, photoelectron spectroscopy allows to distinguish a primary electron in an autoionization channel B and a satellite photoelectron in an Auger decay channel C, with a continuous variation of its kinetic energy tracking the variation of photon energy, in contrast with the classical Auger effect following ionization of a core electron. The photon energy dependence of intensity for both primary and satellite lines should generally display the resonant behavior as indicated by formula (47).

As examples of this resonant Auger decay, we shall refer to cases mentioned in the introduction: krypton (or xenon), on one hand,⁴ Ni⁺ (Refs. 1 and 12) and copper,^{5,6} on the other. Both deserve more details as they involve different values of the zero-order dipole transition matrix elements. In the case of krypton, process (A) creates 3d-hole excited states $3d^9 4s^2 4p^6 np$ which converge on 3d thresholds, while processes (B) and (C) are written:

$$(B) \quad 3d^{10} 4s^2 4p^6 \xrightarrow{h\nu} 3d^{10} 4s^2 4p^5 + e^- \quad (d \text{ or } s),$$

$$(C) \quad 3d^{10} 4s^2 4p^6 \xrightarrow{h\nu} 3d^{10} 4s^2 4p^4 np + e^- \quad (d \text{ or } s).$$

Interference of the three processes leads to the observation of a resonant $M_{45} N_{23} N_{23}$ Auger spectrum, as reported by Eberhardt *et al.*,⁴ which involves the various dipole matrix elements

$$\bar{Q}_B^0 = \langle \epsilon d \text{ (or } \epsilon s) | Q | 4p \rangle$$

and

$$\bar{Q}_C^0 = \langle \epsilon d \text{ (or } \epsilon s) | Q | 4p \rangle \langle 4p | np \rangle.$$

Both \bar{Q}_B^0 and \bar{Q}_C^0 are different from zero, although the overlap integral $\langle 4p | np \rangle$ makes \bar{Q}_C^0 much smaller than \bar{Q}_B^0 , with the consequence that Q_μ^0 is never zero for Auger decay channels C, even if we

neglect the first-order interchannel coupling with the autoionization channels B, in other words, if we make the assumption that the prediagonalized states $|\beta E\rangle$ are identical to the asymptotically observable states $|\mu E\rangle$.

On the contrary, in the copper case ($3p^6 3d^{10} 4s$ configuration), the creation of the excited state $3p^5 3d^{10} 4s^2$ and its decay via interference with processes (B) and (C), according to

$$(B) \quad 3p^6 3d^{10} 4s \xrightarrow{h\nu} 3p^6 3d^9 4s + e^- \quad (f \text{ or } p),$$

$$(C) \quad 3p^6 3d^{10} 4s \xrightarrow{h\nu} 3p^6 3d^8 4s^2 + e^- \quad (f \text{ or } p),$$

involve the zero-order dipole matrix elements $\bar{Q}_B^0 = \langle \epsilon f \text{ (or } \epsilon p) | Q | 3d \rangle \neq 0$ and $\bar{Q}_C^0 = \bar{Q}_B^0 \langle 3d | 4s \rangle = 0$ in the determination of the intensities of the resonant $M_{23} M_{45} M_{45}$ Auger lines, so that corresponding Q_μ^0 and $\alpha(\mu E)$ in channels C would be, respectively, zero and infinite, if coupling of Auger decay channels C with autoionization channels B were negligible. In such a case with $\bar{Q}_C^0 = 0$, asymmetry characteristic of the resonant σ_μ for channels C is directly related to the importance of this interchannel coupling, and when the latter may be neglected, formula (47) has to be altered, leading to a Fano profile in channels B only, while a symmetrical Lorentzian profile is displayed by σ_μ in channels C. Before making explicit this modification in the paragraph below, I shall give here an indication of the importance of process (C) relatively to (B), which I have determined in the case of copper.

With this purpose, assuming *LS* coupling and taking into account all channels $3d^8 4s^2 \epsilon f$ (channels $3d^8 4s^2 \epsilon p$ have a minor influence) resulting from the multiplet structure of $3d^8$, I have calculated the contribution of these Auger decay channels to the total linewidth Γ_t for the resonant line $3p^5 3d^{10} 4s^2 2p^0$, using

$$\Gamma_t = 2\pi \sum_{\mu} |H_{\mu}|^2 = 2\pi \left[\sum_B |H_B|^2 + \sum_C |H_C|^2 \right] = \Gamma_t^B + \Gamma_t^C. \quad (49)$$

I will give here the numerical results relative to Γ_t^B , Γ_t^C , and Γ_t , when considering the decay of the $3p^5 3d^{10} 4s^2 2p^0$ line into all Auger channels $3p^6 3d^8 4s^2 \epsilon f^2 p^0$ and all the autoionization channels $3p^6 3d^9 4s \epsilon f$ (and ϵp) $2p^0$:

$$\frac{1}{2} \Gamma_t^C = \frac{14}{15} R_1^2(3p, 3d; 3d, \epsilon_r f) - \frac{8}{35} R_1(3p, 3d; 3d, \epsilon_r f) R_3(3p, 3d; 3d, \epsilon_r f) + \frac{32}{245} R_3^2(3p, 3d; 3d, \epsilon_r f), \quad (50)$$

R_1 and R_3 being Slater integrals, according to the definition

$$R_k(3p, 3d; 3d, \epsilon f) = \int P_{3p}(1) P_{3d}(1) \frac{2r^k}{r^{k+1}} P_{3d}(2) P_{\epsilon f}(2) dr_1 dr_2, \quad (51)$$

with $r_< = \inf(r_1, r_2)$ and $r_> = \sup(r_1, r_2)$, the continuum wave function P_{ef} being normalized per energy unit (one Rydberg). As for the variation with ϵ , the energy of the photoelectron (in Ry), of the integrals R_1 and R_3 which are also involved in the autoionization of $3p^5 3d^{10} 2P^o$ in the various channels $3p^6 3d^8 \epsilon f$ of Ni^+ (and relatively large since they concern a super-Coster-Krönig transition), I have determined it in the same approximations as in the previous work of Combet Farnoux and Ben Amar,¹ in an independent particle approximation (both discrete and continuum wave functions are eigenfunctions of the same Herman and Skillman¹⁴ potential) neglecting multiplet splitting effects; also, I can use the approximation $R_3 \simeq R_1/2$ in the vicinity of the resonant state $3p^5 3d^{10} 4s^2 2P^o$ ($\epsilon_r \simeq 4.3$ Ry). In this same work,¹ the same approximations to evaluate the linewidth corresponding to the decay of $3p^5 3d^{10} 2P^o$ for Ni^+ have doubled the value obtained with a sophisticated model including both intra- and interchannel coupling and multiplet splitting. With the assumption that overestimation will be of the same order of magnitude here, we can prove that Γ_t^C is at least 20 times larger than the contribution Γ_t^B which I have also calculated in terms of Slater integrals $R_1(3p, 4s; 3d, \epsilon_r f)$, $R_3(3p, 3d; 4s, \epsilon_r f)$, $R_1(3p, 4s; 3d, \epsilon_r p)$, and $R_1(3p, 3d; 4s, \epsilon_r p)$. Referring to another previous work,¹⁵ these integrals are known to be smaller than those involved in Γ_t^C , so that taking into account all channels $3p^6 3d^9 4s^3 D, {}^1D; \epsilon f$ and $3p^6 3d^9 4s^3 D, {}^1D \epsilon p$ relative to the decay of this $3p^5 3d^{10} 4s^2 2P^o$ excited state, I have established (with $\epsilon_r \simeq 4.8$ Ry)

$$\begin{aligned} \frac{1}{2} \Gamma_t^B = & \frac{4}{9} [R_1^2(3p, 3d; 4s, \epsilon_r p) + R_1^2(3p, 4s; 3d, \epsilon_r p) - R_1(3p, 3d; 4s, \epsilon_r p)R_1(3p, 4s; 3d, \epsilon_r p)] \\ & + \frac{6}{49} R_3^2(3p, 3d; 4s, \epsilon_r f) + \frac{2}{3} R_1^2(3p, 4s; 3d, \epsilon_r f) - \frac{2}{7} R_1(3p, 4s; 3d, \epsilon_r f)R_3(3p, 3d; 4s, \epsilon_r f) \end{aligned} \quad (52)$$

leading to $\Gamma_t^B = 0.0112$ Ry, whereas $\Gamma_t^C = 0.24$ Ry. With $\Gamma_t = 0.25$ Ry, we may conclude that an Auger decay at least 20 times more important than direct autoionization makes this linewidth of the same order of magnitude as that found previously¹ for the autoionizing resonant state $3p^5 3d^{10}$ but more quantitative results would require to take into account some double Auger effects.

3. Case of negligible first-order interchannel coupling

Although our previous studies, as well for Ni^+ (Ref. 1) and Cl (Ref. 16) have shown that this assumption is not valid in photoionization of open subshell systems and several authors^{17,18} studying Auger processes have come to the same conclusions, there is no systematic and quantitative evidence of the importance of this interchannel coupling. The present work brings evidence that neglecting these coupling effects may conceal the asymmetry characteristic of the resonant photoemission cross sections in the Auger decay channels, while taking them into account allows to describe the intensity in any channel (for both primary and satellite lines) with formula (47) in terms of a complex parameter $\alpha(\mu E)$ characteristic of each channel and whose variation is given by (45). However, the limit case of no interchannel coupling must be examined here, insofar as some authors^{19,20} have considered only this approximation, within a simplified formalism.

Let us remark first that this approximation implies that the matrix $\tilde{T}_{\beta\mu}(E)$ becomes the unit matrix $\delta_{\beta\mu}$, and both H_μ/Q_μ^0 and $\alpha(\mu E)$ are real numbers. Also, as a result of the prediagonalized states $|\beta E\rangle$ being identical to the asymptotically observable states $|\mu E\rangle$, some notations can be modified:

$$\begin{aligned} |H_\mu|^2 = & V_{1\mu}^2 = \Gamma_\mu/2\pi, \\ |1E\rangle = & \frac{1}{V_t} \sum_\mu V_{1\mu} |\mu E\rangle, \end{aligned} \quad (53)$$

the notation $\psi_{\mu E}^o$ being kept to represent the incoming-wave-normalized counterpart of the standing-wave-normalized states $|\mu E\rangle$. Within this simplified formalism, (41), (44), and (46) which give the dipole transition matrix element in each channel are still valid, and the general formula (47) of the photoemission cross section becomes

$$\sigma_\mu \propto |Q_\mu^0|^2 \left[1 + \alpha^2 \frac{q^2 + 1}{\epsilon^2 + 1} + 2\alpha \frac{\epsilon q - 1}{\epsilon^2 + 1} \right] \quad (54)$$

exhibiting the asymmetry of a Fano profile, provided α is not zero or infinite. Indeed, this latter possibility occurs when Q_C^0 is zero, i.e., in cases like Ni^+ or copper,^{5,6,12} where the shake-up process introduces an electron with an angular momentum different from that of the electron which participates to the direct ionization. These cases are the only ones where negligible interchannel coupling assumption makes Q_μ^0 rigorously zero

and α infinite, leading to a Lorentzian profile in the Auger channels:

$$\sigma_{\mu} \propto \frac{\Gamma_{\mu}}{\Gamma_t} \langle 1E | Q | 0 \rangle^2 \frac{q^2 + 1}{\epsilon^2 + 1}, \quad (55)$$

which leads to a very simple expression for the branching ratio relative to two Auger channels, μ_1 and μ_2 :

$$\gamma_{\mu_1, \mu_2} = \frac{\Gamma_{\mu_1}}{\Gamma_{\mu_2}},$$

and more generally

$$\gamma_{P, Q} = \frac{\sum_{\mu_1 \in P} \Gamma_{\mu_1}}{\sum_{\mu_2 \in Q} \Gamma_{\mu_2}}, \quad (56)$$

when two groups P and Q of photoelectrons with different energies corresponding to two states of the residual core are measured in the vicinity of an isolated resonance.

In short, if μB notation concerns direct autoionization channels and μC is reserved to Auger decay channels, (54) can be used to parametrize the partial cross section relative to both primary and Auger satellite lines when Q_c^0 is different from zero: Both exhibit an asymmetric profile, although the asymmetry characteristic is pretty weak for most satellites, within the framework of negligible interchannel coupling approximation. But when Q_c^0 is zero, formula (55) must be used to reproduce the Lorentzian resonant profile of Auger satellites. An alternative form for (55) may be written:

$$\sigma_{\mu C} \propto \frac{\Gamma_{\mu C}}{\Gamma_t^2} 2\pi \left[\sum_{\mu B} H_{\mu B}^* Q_{\mu B}^0 \right]^2 \frac{q^2 + 1}{\epsilon^2 + 1}. \quad (57)$$

Since Wendin¹⁹ and Yafet²⁰ have treated in this approximation only the case of two channels μB and μC with $Q_c^0 = 0$, it is interesting to show that their formulas are particular cases of (54), (55), and (57) above (see Appendix A).

B. Resonant behavior of partial cross sections when many resonances interfere via many autoionization and Auger decay channels

After the study of an isolated resonance, we must consider now those cases of inner-shell excitation where no potential barrier keeps the other members of a series outside the inner well, but also foresee the complex problem arisen by several resonant series converging on various nearby

thresholds. In this general case, we return to formula (21) and define for each modified discrete state $|\bar{\Phi}_n\rangle$ a new continuum $|nE\rangle$ involving the whole interaction with the resonant state n , such as

$$|nE\rangle = \frac{1}{W_{nt}} \sum_{\beta} W_{n\beta} |\beta E\rangle, \quad (58)$$

$$\frac{1}{2} \Gamma_{nt} = \pi W_{nt}^2 = \langle nE | H | \bar{\Phi}_n \rangle^2 = \pi \sum_{\beta} W_{n\beta}^2, \quad (59)$$

$$q_n = \frac{\langle \bar{\Phi}_n | Q | 0 \rangle}{\pi W_{nt} \langle nE | Q | 0 \rangle} = \frac{\langle \bar{\Phi}_n | Q | 0 \rangle}{\pi \sum_{\beta} W_{n\beta} d_{\beta}}, \quad (60)$$

$$d_{\beta} = \langle \beta E | Q | 0 \rangle,$$

so that

$$Q_{\mu}^0 = \sum_{\beta} A_{\beta\mu}^0 d_{\beta}. \quad (61)$$

Hence, the dipole matrix element relative to any channel μ is written:

$$Q_{\mu} = \sum_{\beta\beta'} Z_{\beta\beta'}^* \left[\sum_n \frac{\pi q_n}{E - \bar{E}_n} W_{n\beta} W_{n\beta'} + \delta_{\beta\beta'} \right] d_{\beta}. \quad (62)$$

It is not easy to invert the $(I - iK)$ matrix to find the normalization matrix Z which presents a pretty complicated energy dependence in these cases where K is not a diagonal matrix. It would be a more direct way to solve the problem by diagonalizing K to obtain its eigenvalues $-\tan\Delta_l$ such as

$$-\tan\Delta_l = \sum_n \frac{\frac{1}{2} \Gamma_{nl}}{E - \bar{E}_n} = \sum_n \frac{1}{\epsilon_{nl}} = \frac{1}{\epsilon_l}, \quad (63)$$

but we thus define new resonance states which have nothing to do with the initial excited states which we are interested in.

If the various continua $|nE\rangle$ for each n are mutually orthogonal, there is no interaction between the resonances due to coupling with the continua and each one may be treated as a single, isolated resonance imbedded in its own continuum. But in the most general case of inner-shell excitation where both autoionization and Auger decay are competing, these continua will not be orthogonal, and a rigorous treatment would require to take into account interference between neighboring reso-

nances via the interference matrix $\Theta_{n,n'}$ between the $|nE\rangle$ continua, introduced by Mies³:

$$\Theta_{n,n'}\delta(E-E') = \langle nE | n'E' \rangle \\ = \frac{1}{\sqrt{\Gamma_{nt}\Gamma_{n't}}} \sum_{\beta} W_{n\beta}W_{n'\beta}. \quad (64)$$

While $\Theta_{n,n'}=1$ for $n=n'$ implies that the overlap is maximum, i.e., all resonances decay into the same continuum, $|1E\rangle$, $\Theta_{n,n'}=\delta_{n,n'}$ corresponds to no overlap, i.e., the continua $|nE\rangle$ for each n are orthogonal. These two cases are the only ones (outside the case of an isolated resonance) where inversion of the matrix $(I-iK)$ may be achieved analytically, but the examples presented above should rather be relevant to $\Theta_{n,n'}\neq 0$ for $n\neq n'$, since even if the Auger decay channels C are different for each resonant state (which means that double Auger processes would be negligible), the autoionization channels B are the same. Returning to the example of Ni^+ , there is no doubt that the reduction of Γ_t when going from $3p^53d^{93}P^o4s^2P^o$ to $3p^53d^{93}P^o5s^2P^o$ is due to the decreasing contribution Γ_t^B of the autoionization channels $3p^63d^8\epsilon f$ (and ϵp) while the contribution Γ_t^C of the Auger channels is left unchanged, the channels $3p^63d^75s\epsilon f$ (and ϵp) playing the role of channels $3p^63d^74s\epsilon f$ before.

Actually, as mentioned by Fano and Cooper² and observed in photoabsorption by Codling and Madden,²¹ only the first lines of a series show up, the other ones eventually merging with one another because of the ratio of linewidth to line separation which increases indefinitely with increasing n . Therefore, if Auger decay (which is, in fact, independent of n) is already predominant over direct autoionization (which is getting smaller and smaller with increasing n) for the first line, the width of further lines in the series may result from Auger decay channels only, even if the coupling between Auger and autoionization channels is not negligible. In these cases, $\Theta_{n,n'}$ (for $n\neq n'$) may be small enough to allow for neglecting the off-diagonal couplings in the K matrix so that we can make the assumption (at first-order approximation) that there is no overlap between resonances and thus obtain a pretty good idea of the resonant behavior in each channel. I will devote Sec. III B 1 to this special case of direct diagonalization of the K matrix, without giving more attention to the other special case where all resonances decay into the same continuum $|1E\rangle$, insofar it is relevant to the Rydberg series which converge on the first ioniza-

tion thresholds when Auger decay is energetically forbidden and the linewidths are due to autoionization only.

1. There is no overlap between any two resonances

As a consequence of $\Theta_{n,n'}=0$ when $n\neq n'$, and $\Theta_{n,n'}=1$ for $n=n'$, there is no need to replace the initial $|F_n\rangle$ states by a new set of $|\Phi_n\rangle$ states, as we did in the general case treated in Sec. II B above. In fact, because the $|nE\rangle$ continua for different n are orthogonal, transitions between the $|F_n\rangle$ states via the continua cannot occur. Therefore, for each $|\bar{F}_n\rangle$ there is one continuum $|n_1E\rangle$ and one eigenstate $|n_1E\rangle$ which is a linear combination of $|\bar{F}_n\rangle$ and $|n_1E\rangle$ according to (28), i.e., the same eigenstate as in the case of an isolated resonance:

$$|n_1E\rangle = \frac{\sin(-\Delta_n)}{\pi V_{nt}} |\bar{F}_n\rangle + \cos(-\Delta_n) |n_1E\rangle. \quad (65)$$

The other $|n_\lambda E\rangle$ ($2\leq\lambda\leq N$) are simply linear combinations of $|\beta E\rangle$ states, as explained in Sec. II C above. All the formulas of the paragraph are still valid here, and I will recall only

$$\frac{1}{2}\Gamma_{nt} = \pi V_{nt}^2 = \pi \langle n_1E | H | F_n \rangle^2 = \pi \sum_{\beta} V_{n\beta}^2, \quad (66)$$

$$|n_1E\rangle = \frac{1}{V_{nt}} \sum_{\beta} V_{n\beta} |\beta E\rangle, \quad (67)$$

with the condition

$$\sum_{\beta} V_{n\beta} V_{n\beta} = 0 \quad (68)$$

which is equivalent to write that the interference matrix $\Theta_{n,n'}$ has no off-diagonal elements. In this case, determining the wave function $\psi_{\mu E}^-$ describing an observable channel is straightforward and the inversion of the $(I-iK)$ matrix can be as easily achieved as in the case of one isolated resonance treated in Sec. III A 1 above. I will not reproduce the details of the calculations but I shall give only the result

$$\psi_{\mu E}^- = \psi_{\mu E}^0 + \sum_n \frac{H_{n\mu}^*}{V_{nt}} \left[\frac{|\bar{F}_n\rangle}{\pi V_{nt}} + i |n_1E\rangle \right] \frac{1}{\epsilon - i}, \quad (69)$$

with

$$H_{n\mu} = \langle \psi_{\mu E}^0 | H | F_n \rangle = \sum_{\beta} A_{\beta\mu}^0 V_{n\beta}. \quad (70)$$

In the same way, we can generalize (41) to write the corresponding expression giving Q_{μ} , the dipole transition matrix element,

$$Q_{\mu} = Q_{\mu}^0 + \sum_n \frac{H_{n\mu}}{V_{nt}} \frac{q_n - i}{\epsilon_n + i} \langle n_1 E | Q | 0 \rangle \quad (71)$$

or an alternative expression if we introduce the quantity $\alpha_n(\mu E)$ for each n , according to formula (45) above:

$$Q_{\mu} = Q_{\mu}^0 \left[1 + \sum_n \alpha_n(\mu E) \frac{q_n - i}{\epsilon_n + i} \right]. \quad (72)$$

Both formulas [(71) and (72)] show that in this case the expression of the photoemission cross section σ_{μ} in each μ channel would be very complicated, because of the summation over all the autoionizing states. Actually, the determination of $|Q_{\mu}|^2$ involves many interference terms between the various resonant contributions from different decaying states, in addition to the summation over n :

$$\sum_n \left[|\alpha_n|^2 \frac{q_n^2 + 1}{\epsilon_n^2 + 1} + 2 \operatorname{Re} \alpha_n \frac{\epsilon_n q_n - 1}{\epsilon_n^2 + 1} + 2 \operatorname{Im} \alpha_n \frac{\epsilon_n + q_n}{\epsilon_n^2 + 1} \right].$$

These interference terms make the cross section strongly dependent on the intervals between the resonant states and explain why it is impossible to distinguish the contribution of each resonance in a channel, beyond a certain value of n in a series. However, it is of interest to notice that they are a consequence of the interchannel coupling, since neglecting it makes the summation over n disappear in both (71) and (72) which take the simplified formulation

$$Q_{\mu} = Q_{\mu}^0 \left[1 + \alpha_n(\mu E) \frac{q_n - i}{\epsilon_n + i} \right], \quad (73)$$

n defining now the only resonant state which decays into the channel μ . In agreement with the approximation of no overlap between resonances, n means the first line (which is the most intense) in the autoionization channels, while each Auger channel involves the appropriate line which decays into it. For Auger channels such as $Q_{\mu}^0 = 0$, as ex-

plained in Sec. III A 2, formula (73) must be written

$$Q_{\mu} = \frac{V_{n\mu}}{V_{nt}} \frac{q_n - i}{\epsilon_n + i} \langle n_1 E | Q | 0 \rangle \quad (74)$$

leading to a Lorentzian profile for σ_{μ} , analogous to the one given by (55).

As an important conclusion of this section, in case of no overlap, while the approximation of no first-order interchannel coupling lets only one line appear in each channel, the introduction of this coupling, even small, allows to find slight extra structures due to neighboring resonances in any channel. However, in both approximations, the total photoabsorption cross section (summation over all channels μ) would be the sum of resonant profiles superimposed on a background.

2. Discussion

If the approximation of no overlap between resonances may be valid for the last members of series which converge on the next ionization thresholds, the rigorous treatment of the first resonances decaying into both autoionization and Auger decay channels will require to take into account the off-diagonal coupling terms of the K matrix which were neglected in Sec. III B 1. It is easy to predict the behavior of σ_{μ} in any channel for those cases where a prediagonalization of the resonant states concerned is possible. This prediagonalization provides n new states to which we give the new label l to indicate that, although a configuration designation is often not applicable, each new l resonant state decays into a $|l_1 E\rangle$ new continuum which has no overlap with the others; in fact, these new continua $|l_1 E\rangle$ are obtained as the result of the same prediagonalization, since the diagonalized interaction is the same as for the discrete states. The formulas of Sec. III B 1 may be applied to these prediagonalized resonant states and continua, and since the observable channels may be considered as linear combinations of these new continua (without any overlap with each other), we can expect that the major effect of the off-diagonal coupling terms of the K matrix consists in shifting and intensifying these extra structures due to neighboring resonances which interchannel interactions let appear in each channel. A unified treatment, as developed by Fano²² and derived from the multichannel quantum-defect theory proposed by Seaton²³ could be of great help in such complex cases, but to my

knowledge, it has only been applied so far to perturbed series approaching the first ionization limits²⁴ when autoionization of the inner core cannot occur.

IV. GENERAL DISCUSSION AND CONCLUSIONS

This study uses the time-independent multichannel scattering theory in a way which follows the configurational-interaction approach^{3,9} closely enough to serve as a background of new models using recent computational approaches of both relativistic and nonrelativistic continuum wave functions. This formalism has often been used in the treatment of resonances near threshold,^{25,26} as well for radiative as nonradiative processes,²⁷ with the advantage of separating the nonresonant background contribution from the resonant one. The present work shows the great interest of such a treatment of the resonant Auger effect to the extent that it points out the importance of coupling the direct autoionization and the Auger decay channels when parametrizing the resonant behavior of the photoemission cross sections in order to interpret the core-level spectra, as observed in photoelectron spectroscopy. In short, three parameters $\alpha_n(\mu E)$, q , and Q_μ^0 are necessary to determine the behavior of any kind of photoabsorption process in any channel μ , in the neighborhood of a particular n -resonant state; their values give much information about the relative intensities of the decay into the autoionization and Auger channels as well as the importance of the coupling between these two types of channels. Although there is no apparent relationship between these relative intensities of decay and the importance of the coupling between the corresponding channels, two main classes may be distinguished.

(1) $\alpha_n(\mu E)$ taking complex values in all channels corresponds to an important interchannel coupling which leads to an asymmetric Fano profile for the behavior of photoemission cross sections in both autoionization and Auger channels; the q value depends on both types of decay.

(2) $\alpha_n(\mu E)$ becoming a real number in all channels means that the first-order interchannel effects are negligible, and only the autoionization channels may exhibit a pronounced asymmetry of the partial cross section, whereas a nearly symmetric shape of the resonance in an Auger channel gives evidence of a very small Q_μ^0 (off-resonance dipole matrix element). The limit case of a true Lorentzian line corresponds to Q_μ^0 rigorously zero and α infinite.

Within this category, small Q_μ^0 's may occur also for autoionization channels and lead to a nearly symmetric profile for all partial cross sections and the photoabsorption spectrum. In all cases, the q parameter of the total absorption profile is close to the value obtained when disregarding the Auger decay. Let us mention that all these conclusions depend on the assumption that the various matrix elements involved in both q and α are slowly varying in the proximity of the resonance.

It would be of great interest to know which category the examples presented in this work belong to. Up to now, no fitting of experimental results has been achieved to determine simultaneously $\alpha(\mu E)$, q , and Q_μ^0 . Actually, such a fitting requires to know the variation of individual partial cross sections as a function of photon energy, and generally, only the branching ratio of different groups of photoelectrons is measured. Starace⁸ has shown that in the special case of only two groups of photoelectrons, the branching ratio within a resonance depends on only two independent parameters which are linear combinations of the various α 's and Q_μ^0 's, so that the latter cannot be determined directly. The present work should be an inducement to experimentalists to determine the absolute values of individual partial cross sections: Work in that area of selective photoexcitation of Auger electrons and exploration of the neighborhood of thresholds and resonances has just begun but deserves further expansion since it offers the opportunity of disentangling the various processes that occur during deexcitation of core vacancies. To be significant, a fitting to theoretical results would require to perform *ab initio* calculations of partial cross sections with a model sophisticated enough to take into account the interchannel coupling. Such calculations are in progress for copper⁶ insofar as the observation⁵ of weak off-resonance satellites (shake-up satellites) is in favor of a certain but weak coupling between autoionization and Auger channels; as mentioned in Sec. III A 2 above, neglecting this coupling would make Q_μ^0 rigorously zero in all Auger channels. In other words, copper corresponds to the first class defined above, with both $\alpha(\mu E)$ and Q_μ^0 complex ($Q_\mu^0 \neq 0$) in all channels μ and these conclusions are independent of including or not the spin-orbit effects, since in copper, the transition is an allowed one (i.e., $^2S \rightarrow ^2P$) and the effect of spin-orbit interactions is to induce a fine-structure splitting between the $^2P_{3/2}$ and $^2P_{1/2}$ final states. Actually Fig. 1 which displays the absorption spectrum of

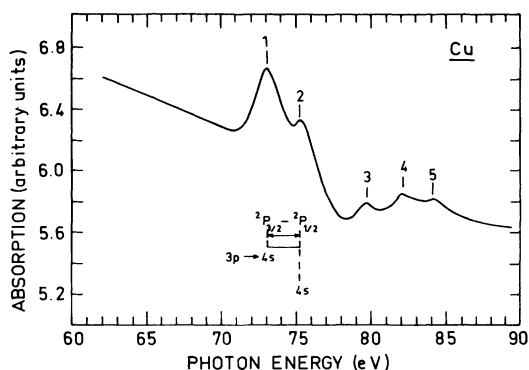


FIG. 1. Absorption spectrum of Cu vapor obtained by Bruhn *et al.* (Ref. 28): peaks 1 and 2 correspond, respectively, to transitions $3p^6 3d^{10} 4s^2 S_{1/2} \rightarrow 3p^5 3d^{10} 4s^2 ({}^2P_{1/2} \text{ and } {}^2P_{3/2})$.

Cu vapor obtained by Bruhn *et al.*²⁸ shows that the resonance $3p^5 3d^{10} 4s^2$ gives rise to two peaks separated by the spin-orbit splitting of the $3p$ hole which is not resolved in recent photoelectron spectroscopy measurements.⁵ By contrast, experimentalists⁴ have observed no shake-up satellite away from the resonance $4d^9 ({}^2D_{5/2}) 6p$ below $4d$ thresholds of Xe, whereas I pointed out in Sec. III A 2 above that Q_μ^0 cannot be zero in a zero-order central field model. This absence of shake-up satellites is in agreement with the nearly Lorentzian shape of the photoabsorption profile for this resonance (at 65 eV) which can be seen in Fig. 2, and for which

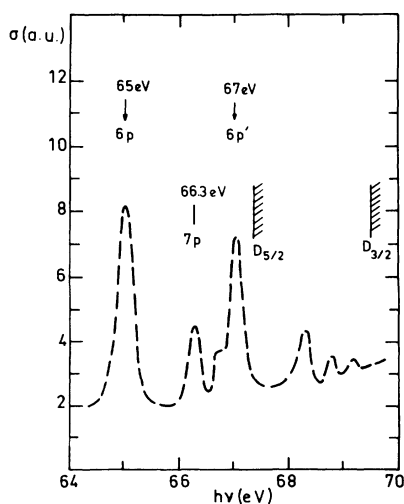


FIG. 2. Absorption spectrum of Xe in the region of the onset of the $4d$ transitions, in arbitrary units, after Eberhardt *et al.* (Ref. 4): the resonance lines $4d^9 5s^2 5p^6 {}^2D_{5/2}$, ${}^2D_{3/2} np$ are superimposed on a background of $5p$ - and $5s$ -electron excitations.

Ederer and Manalis²⁹ found the parameter q very large ($q \approx 200$). In other words, although photoelectron spectroscopy measurements⁴ do not provide us with individual partial cross sections to be parametrized, we can conclude that resonances located below the ${}^2D_{5/2}$ threshold of xenon belong to the second class defined above, with both $\alpha(\mu E)$ and Q_μ^0 real in all channels μ (Q_μ^0 very small and α very large). Like for copper, autoionization is weak relatively to Auger decay, but in addition, the effect of spin-orbit interactions which consists in populating some forbidden transitions makes Q_μ^0 weaker in the autoionization channels and leads to a nearly symmetric profile in all the observable channels. Also, $5s$ and $5p$ cross sections are varying so slowly in this region below $4d$ thresholds that we cannot expect, in agreement with the K matrix models,^{11,30} that coupling both autoionization and Auger channels enhances substantially the small dipole matrix elements in the Auger channels. According to Fig. 2, which displays the absorption spectrum below both ${}^2D_{5/2}$ and ${}^2D_{3/2}$ thresholds of xenon, the resonances which converge into the ${}^2D_{3/2}$ limit appear to be more asymmetric than the others, a remark which is in favor of a larger participation of the allowed transition ${}^1S_0 \rightarrow {}^1P_1$, leading to α smaller and Q_μ^0 not negligible in the autoionization channels.

The examples presented in this work, with the purpose of illustrating the various events, do not imply that these results and conclusions are valid only in the ultraviolet energy range, when the subshells concerned by excitation are not the inner ones. Actually, resonant Auger effect has been observed recently in the x-ray range, below $2p$ thresholds of xenon³¹; in fact, even if autoionization is often negligible relatively to Auger decay at these high energies, the present work keeps its validity for those cases of important spin-orbit effects, whose illustration may be given by the $M_{4,5}$ spectrum of lanthanum, extensively studied by several techniques³² and where the dominant features are the $3d_{5/2,3/2} \rightarrow 4f$ lines occurring below the $3d$ thresholds, as shown in Fig. 3. While the $3d^9 4f {}^3D_1$ excited state decays essentially via Auger process and the corresponding $3d_{5/2} \rightarrow 4f$ line is located below the M_5 thresholds, the other line ($3d_{3/2} \rightarrow 4f {}^1P_1$) is observed above it, which means that the opening of a new channel into which this $3d^9 4f {}^1P_1$ resonant state decays via autoionization accounts for the extra broadening observed when we compare the widths of the two lines 3D_1 and 1P_1 as well as the asymmetry of the second line. This conclusion has been used recent-

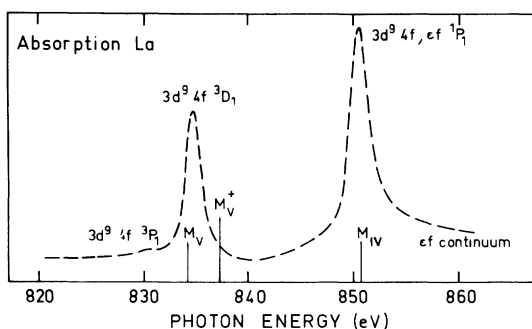


FIG. 3. Absorption spectrum of metallic La [after Mariot and Karnatak (Ref. 34)]: $M_{IV}M_V$ are the original thresholds from Mariot and Karnatak (Ref. 34), but a more recent value for M_V , given by Kanski *et al.* (Ref. 32), is marked with a cross.

ly by Connerade and Karnatak³³ to provide a relation between the breadths of the absorption lines and the change of relative intensities from absorption to emission, as pointed out previously by Mariot and Karnatak.³⁴ Although Connerade and Karnatak³³ obtain a pretty good agreement with experiment³⁴ when assuming no interference between autoionization and Auger decay, photoelectron spectroscopy measurements would be welcome to confirm the relative importance of autoionization and Auger decay and how each process is altered by the other one. Also, *ab initio* calculations of the α and Q_μ^0 parameters would provide a test of theoretical models for incorporating spin-orbit effects and other relativistic interactions into atomic collision computations relative to the ion La^{3+} (xenonlike configuration).

Returning to the other example (resonant state $3p^5 3d^{10} 4s^2$ of Cu), for which I have shown the importance of both autoionization and Auger decay, I have anticipated that introducing the coupling of all channels may make asymmetric the profile of resonances in Auger channels, but a more dramatic alteration must be expected for those elements around Ag (or Au) which involve autoionization into $4d$ (or $5d$) ionization channels which exhibit a sharp shape resonance. The latter remark should be still valid for $5d$ excitations in actinides, where $5d \rightarrow 5f$ transitions produce resonant states below and above O_5O_4 thresholds, as confirmed by recent photoemission experiments of Iwan *et al.*³⁵ for uranium metal, which point out the existence of asymmetric satellites around the $5d$ thresholds. As a conclusion, I want to stress the interest of the present theoretical work for solid-state experimen-

talists^{35,36} who have observed either a giant resonance enhancement of the primary lines or two-electron resonant satellites accounted for recently by atomic Auger processes, in many metals and compounds, using synchrotron radiation and photoemission techniques.

The author wishes to express her gratitude to Professor U. Fano for a critical and enlightening discussion about this manuscript before submitting it and Dr. D. L. Ederer for stimulating discussions during his one-year stay in Orsay.

APPENDIX

The particular case of only two channels μB (autoionization) and μC (Auger decay) has been treated independently by Wendin¹⁹ and Yafet²⁰ assuming negligible interchannel interactions and $Q_{\mu C}^0 = 0$, so that the formulas obtained by these authors for $Q_{\mu B}$, $Q_{\mu C}$, $\sigma_{\mu B}$, and $\sigma_{\mu C}$ are particular cases of (44), (54), (55), and (57) above, and are easily written:

$$Q_{\mu B} = Q_{\mu B}^0 \left[1 + \frac{\Gamma_{\mu B}}{\Gamma_t} \frac{q-i}{\epsilon+i} \right] \quad (\text{A1})$$

$$Q_{\mu C} = 2\pi \frac{H_{\mu C} H_{\mu B}}{\Gamma_t} \frac{q-i}{\epsilon+i} Q_{\mu B}^0,$$

$$\sigma_{\mu B} \propto |Q_{\mu B}^0|^2 \left[1 + \frac{\Gamma_{\mu B}^2}{\Gamma_t^2} \frac{q^2+1}{\epsilon^2+1} + 2 \frac{\Gamma_{\mu B}}{\Gamma_t} \frac{\epsilon q-1}{\epsilon^2+1} \right], \quad (\text{A2})$$

$$\sigma_{\mu C} \propto |Q_{\mu B}^0|^2 \frac{\Gamma_{\mu B} \Gamma_{\mu C}}{\Gamma_t^2} \frac{q^2+1}{\epsilon^2+1}. \quad (\text{A3})$$

In this particular case which excludes any multiplet splitting, σ_μ for the autoionization channel depends on the real value $\alpha = \Gamma_{\mu B} / \Gamma_t$, and since $\Gamma_t = \Gamma_{\mu B} + \Gamma_{\mu C}$, we can point out that introducing the Auger decay influences $Q_{\mu B}$ and $\sigma_{\mu B}$ via a shorter lifetime of the resonant state. As for the Lorentzian profile of the intensity in an Auger decay channel, formula (A3) shows that it depends also on α via the relation

$$\frac{\Gamma_{\mu B} \Gamma_{\mu C}}{\Gamma_t^2} = \alpha(1-\alpha). \quad (\text{A4})$$

Moreover, the addition of $\sigma_{\mu B}$ and $\sigma_{\mu C}$ leads to a total absorption cross section σ_t according to the following expression:

$$\sigma_t \propto |Q_{\mu B}^0|^2 \left[\frac{\Gamma_{\mu C}}{\Gamma_t} + \frac{\Gamma_{\mu B}}{\Gamma_t} \frac{(q+\epsilon)^2}{\epsilon^2+1} \right], \quad (\text{A5})$$

which is identical to Fano's formula,⁹ with

$$\begin{aligned} \sigma_b &\propto |Q_{\mu B}^0|^2 \frac{\Gamma_{\mu C}}{\Gamma_t} \\ \sigma_a &\propto |Q_{\mu B}^0|^2 \frac{\Gamma_{\mu B}}{\Gamma_t}, \end{aligned} \quad (\text{A6})$$

and ρ^2 the correlation coefficient such as

$$\rho^2 = \frac{\sigma_a}{\sigma_a + \sigma_b} = \frac{\Gamma_{\mu B}}{\Gamma_t} = \alpha_{\mu B} \quad (\text{A7})$$

is in agreement with the assumption that a low value of ρ^2 shows that autoionization leads to different final states of the residual ion than direct ionization. In other words, in the particular case of only two channels, with the off-resonance transition matrix element $Q_{\mu C}^0$ equal to zero, both the asymmetric behavior of $\sigma_{\mu B}$ and the Lorentzian shape of $\sigma_{\mu C}$ are determined by only three parameters: $\alpha_{\mu B}$, $Q_{\mu B}^0$, and q . Even in this case, it is clear that the system remembers for a while how the core hole was created and, in particular, what photon energy was used so that its decay could not be treated independently of the photoabsorption process. Equivalent formulas have been obtained by Åberg²⁷ in his general study of the decay of metastable states.

-
- ¹F. Combet Farnoux and M. Ben Amar, Phys. Rev. A **21**, 1975 (1980).
²U. Fano and J. W. Cooper, Phys. Rev. A **137**, 1364 (1965).
³F. H. Mies, Phys. Rev. **175**, 164 (1968).
⁴W. Eberhardt, G. Kalkoffen, and C. Kunz, Phys. Rev. Lett. **41**, 156 (1978).
⁵D. Chandris, C. Guillot, G. Chauvin, J. Lecante, and Y. Petroff, Phys. Rev. Lett. **47**, 1273 (1981).
⁶F. Combet Farnoux and M. Ben Amar, *Abstracts of the European Conference on Atomic Physics*, April, 1981, Heidelberg, West Germany (Physikalisches Institut, Heidelberg, 1981), Vol. 1, p. 138; F. Combet Farnoux (unpublished).
⁷A. F. Starace, Phys. Rev. B **5**, 1773 (1972).
⁸A. F. Starace, Phys. Rev. A **16**, 231 (1977).
⁹U. Fano, Phys. Rev. **124**, 1866 (1961).
¹⁰N. M. Kabachnik and I. P. Sazhina, J. Phys. B **9**, 1681 (1976).
¹¹U. Fano and J. W. Cooper, Rev. Mod. Phys. **40**, 441 (1968); J. L. Dehmer, Phys. Fenn. **9**, (Suppl. S1), 60 (1974).
¹²F. Combet Farnoux, *Extended Abstracts of the Sixth International Conference on Vacuum Ultraviolet Radiation Physics, June, 1980, Charlottesville, Virginia*, (University of Charlottesville Press, Charlottesville, 1980), Vol. I, p. 101.
¹³M. O. Krause and T. A. Carlson, Phys. Rev. **149**, 52 (1966).
¹⁴F. Herman and S. Skillman, *Atomic Structure Calculations* (Prentice-Hall, Englewood Cliffs, N.J., 1963).
¹⁵M. Ben Amar, Thesis, Orsay, 1979 (unpublished).
¹⁶M. Lamoureux and F. Combet Farnoux, J. Phys. **40**, 545 (1979).
¹⁷G. Howat, T. Åberg, and O. Goscinski, J. Phys. B **11**, 1575 (1978).
¹⁸M. Ohno and G. Wendin, J. Phys. B **12**, 1305 (1979).
¹⁹G. Wendin, *Photoionization of Atoms and Molecules*, edited by B. D. Buckley (Science Research Council, Daresbury, 1978) (Daresbury Laboratory Report No. DL/SC1/R11, p. 1).
²⁰Y. Yafet, Phys. Rev. B **21**, 5023 (1980).
²¹K. Codling and R. P. Madden, Phys. Rev. Lett. **12**, 106 (1964).
²²U. Fano, Phys. Rev. A **2**, 353 (1970).
²³M. J. Seaton, Proc. Phys. Soc. London, Sec. A **88**, 801 (1966).
²⁴K. T. Lu, Phys. Rev. A **4**, 579 (1971); C. M. Lee and K. T. Lu, *ibid.* **8**, 1241 (1973); K. T. Lu, J. Opt. Soc. Am. **64**, 706 (1974).
²⁵D. E. Ramaker and D. M. Schrader, Phys. Rev. A **9**, 1980 (1974).
²⁶R. K. Nesbet, J. Phys. B **13**, L193 (1980).
²⁷T. Åberg, Phys. Scr. **21**, 495 (1980).
²⁸R. Bruhn, B. Sonntag, and H. W. Wolff, J. Phys. B **12**, 203 (1979).
²⁹D. L. Ederer and M. Manalis, J. Opt. Soc. Am. **65**, 634 (1975).
³⁰A. F. Starace, Phys. Rev. A **2**, 118 (1970).
³¹G. S. Brown, M. H. Chen, B. Crasemann, and G. E. Ice, Phys. Rev. Lett. **45**, 1937 (1980).
³²C. Bonnelle, R. C. Karnatak, and J. Sugar, Phys. Rev.

- A 9, 1920 (1974); J. Kanski, P. O. Nilson, and I. Curelaru, J. Phys. F 6, 1073 (1976); J. Kanski and P. O. Nilson, Phys. Rev. Lett. 43, 1185 (1979).
- ³³J. P. Connerade and R. C. Karnatak, J. Phys. F 11, 1539 (1981).
- ³⁴J. M. Mariot and R. C. Karnatak, J. Phys. F 4, L233 (1974).
- ³⁵M. Iwan, E. E. Koch, and F. J. Himspel, Phys. Rev. B 24, 613 (1981).
- ³⁶C. Guillot, Y. Ballu, J. Paigné, J. Lecante, K. P. Jain, P. Thiry, R. Pinchaux, Y. Petroff, and L. M. Falicov, Phys. Rev. Lett. 39, 1632 (1977); W. Lenth, F. Lutz, J. Barth, G. Kalkoffen, and C. Kunz, *ibid.* 41, 1185 (1978); M. Iwan, F. J. Himpsel, and D. E. Eastman, *ibid.* 43, 1829 (1979); G. P. Williams and G. J. Lapeyre, Phys. Rev. B 20, 5280 (1979).